Supplementary Information

Substituent effects and the role of negative hyperconjugation on siloxycarbene rearrangements

*Paul G. Loncke and Gilles H. Peslherbe**

Centre for Research in Molecular Modeling and

Department of Chemistry and Biochemistry

Concordia University

Montréal, Québec, Canada H4B 1R6

List of Tables

List of Figures

Table S 1 Selected MP2/6-311+G(2d,p) geometric parameters of the minimum-energy conformers of methoxy(substituted-siloxy)carbenes.[a]

X	σ_I	∠C6O7Si	C1-O2	O2-C6	C6-O7	O7-Si
			A(X)			
H	0.03	111.5	1.442	1.313	1.333	1.705
NH_2	0.08	111.9	1.441	1.318	1.326	1.717
CCH	0.22	110.1	1.443	1.312	1.333	1.702
SH	0.30	109.3	1.444	1.311	1.333	1.705
OH	0.33	110.1	1.442	1.313	1.330	1.706
Cl	0.42	105.9	1.445	1.307	1.335	1.699
F	0.45	105.8	1.444	1.308	1.333	1.697
CN	0.51	106.7	1.446	1.304	1.341	1.693
			B(X)			
H	0.03	109.8	1.456	1.307	1.345	1.710
NH_2	0.08	110.1	1.457	1.312	1.337	1.723
CCH	0.22	108.6	1.460	1.306	1.345	1.700
SH	0.30	106.8	1.461	1.303	1.348	1.704
OH	0.33	107.5	1.458	1.308	1.341	1.713
Cl	0.42	102.7	1.462	1.302	1.346	1.706
F	0.45	101.3	1.461	1.302	1.342	1.707
CN	0.51	103.6	1.463	1.298	1.352	1.700
			C(X)			
H	0.03	124.5	1.442	1.335	1.321	1.710
NH_2	0.08	125.8	1.441	1.330	1.318	1.722
CCH	0.22	124.0	1.443	1.336	1.323	1.711
SH	0.30	124.2	1.444	1.336	1.324	1.711
OH	0.33	125.1	1.442	1.338	1.321	1.710
Cl	0.42	123.2	1.445	1.336	1.326	1.702
F	0.45	123.7	1.444	1.337	1.324	1.696
CN	0.51	122.3	1.446	1.333	1.329	1.701

[a] Bond angles and interatomic distances are in degrees and Å, respectively.

Table S 2 Selected MP2/6-311+G(2d,p) geometric parameters of the transition states for 1,2-silyl migration and decarbonylation of methoxy(substituted-siloxy)carbenes.[a]

X	σ_I	∠C6O7Si	C1-O2	O2-C6	C6-O7	O7-Si
			TS_{AD}(X)			
H	0.03	74.1	1.435	1.311	1.285	1.900
NH_2	0.08	78.7	1.445	1.313	1.289	1.845
CCH	0.22	72.5	1.447	1.310	1.282	1.912
SH	0.30	74.8	1.448	1.306	1.287	1.873
OH	0.33	73.9	1.446	1.310	1.282	1.898
Cl	0.42	68.7	1.448	1.307	1.274	1.955
F	0.45	68.1	1.447	1.310	1.271	1.970
CN	0.51	70.6	1.450	1.303	1.282	1.918
			TS_{BE}(X)			
H	0.03	74.2	1.459	1.305	1.296	1.898
NH_2	0.08	79.6	1.458	1.307	1.301	1.834
CCH	0.22	72.4	1.460	1.304	1.292	1.909
SH	0.30	75.6	1.461	1.301	1.300	1.859
OH	0.33	74.9	1.459	1.304	1.294	1.882
Cl	0.42	68.5	1.460	1.301	1.294	1.882
F	0.45	69.3	1.459	1.303	1.283	1.942
CN	0.51	70.6	1.462	1.297	1.292	1.914
			TS_{CH}(X)			
H	0.03	103.3	1.439	1.475	1.253	1.951
NH_2	0.08	105.0	1.438	1.446	1.263	1.899
CCH	0.22	103.4	1.440	1.477	1.253	1.937
SH	0.30	103.4	1.441	1.459	1.260	1.920
OH	0.33	103.5	1.439	1.469	1.257	1.937
Cl	0.42	103.7	1.445	1.447	1.266	1.879
F	0.45	103.8	1.442	1.445	1.266	1.882
CN	0.51	102.4	1.443	1.505	1.249	1.934

[a] Bond angles and interatomic distances are in degrees and Å, respectively.

Table S 3 MP2/6-311+G(2d,p) bond critical point electronic densities of the ground-state conformers of methoxy(substituted-siloxy)carbenes.[a]

X	C1-O2	O2-C6	C6-O7	O7-Si
		A(X)		
H	1.596	2.152	2.070	0.811
NH_2	1.607	2.126	2.101	0.791
CCH	1.593	2.159	2.066	0.827
SH	1.590	2.161	2.066	0.822
OH	1.598	2.149	2.082	0.818
Cl	1.583	2.181	2.062	0.843
F	1.586	2.178	2.073	0.846
CN	1.573	2.200	2.034	0.853
		B(X)		
H	1.548	2.164	2.002	0.800
NH_2	1.562	2.138	2.036	0.780
CCH	1.543	2.172	1.999	0.818
SH	1.536	2.186	1.989	0.824
OH	1.552	2.162	2.021	0.806
Cl	1.532	2.197	2.007	0.828
F	1.535	2.195	2.028	0.825
CN	1.521	2.216	1.976	0.839
		C(X)		
H	1.587	2.036	2.089	0.781
NH_2	1.599	2.013	2.108	0.769
CCH	1.584	2.034	2.083	0.798
SH	1.570	2.062	2.105	0.805
OH	1.589	2.026	2.089	0.795
Cl	1.573	2.036	2.063	0.822
F	1.577	2.029	2.073	0.830
CN	1.561	2.048	2.053	0.824

[a] BCP electronic densities are in e/Å^3 and were obtained from AIM analysis.

Table S 4 MP2/6-311+G(2d,p) bond critical point electronic densities of the transition states for 1,2-silyl migration and decarbonylation of methoxy(substituted-siloxy)carbenes.[a]

X	C1-O2	O2-C6	C6-O7	O7-Si	C6-Si
			TS_{AD}(X)		
H	1.572	2.160	2.381	0.513	0.499
NH_2	1.582	2.151	2.347	0.578	-
CCH	1.567	2.167	2.399	0.511	0.533
SH	1.562	2.185	2.362	0.551	
OH	1.572	2.166	2.387	0.518	0.504
Cl	1.558	2.184	2.442	-	0.605
F	1.566	2.171	2.461	-	0.610
CN	1.547	2.205	2.400	-	0.581
			TS_{BE}(X)		
H	1.532	2.192	2.311	0.512	0.494
NH_2	1.543	2.179	2.270	0.589	
CCH	1.528	2.201	2.333	0.509	0.531
SH	1.524	2.215	2.285	0.564	-
OH	1.537	2.196	2.312	0.531	-
Cl	1.521	2.219	2.381	-	0.608
F	1.528	2.210	2.382	-	0.593
CN	1.508	2.239	2.334	-	0.580
			TS_{CH}(X)		
	C1-O2	O2-C6	C6-O7	O7-Si	O2-Si
H	1.559	1.456	2.533	0.469	0.405
NH_2	1.568	1.560	2.465	0.526	0.351
CCH	1.555	1.448	2.530	0.488	0.417
SH	1.547	1.510	2.486	0.512	0.400
OH	1.558	1.478	2.507	0.485	0.400
Cl	1.519	1.551	2.460	0.555	0.416
F	1.536	1.559	2.457	0.551	0.405
CN	1.534	1.357	2.553	0.489	0.474

[a] BCP electronic densities are in e/Å^3 and were obtained from AIM analysis.

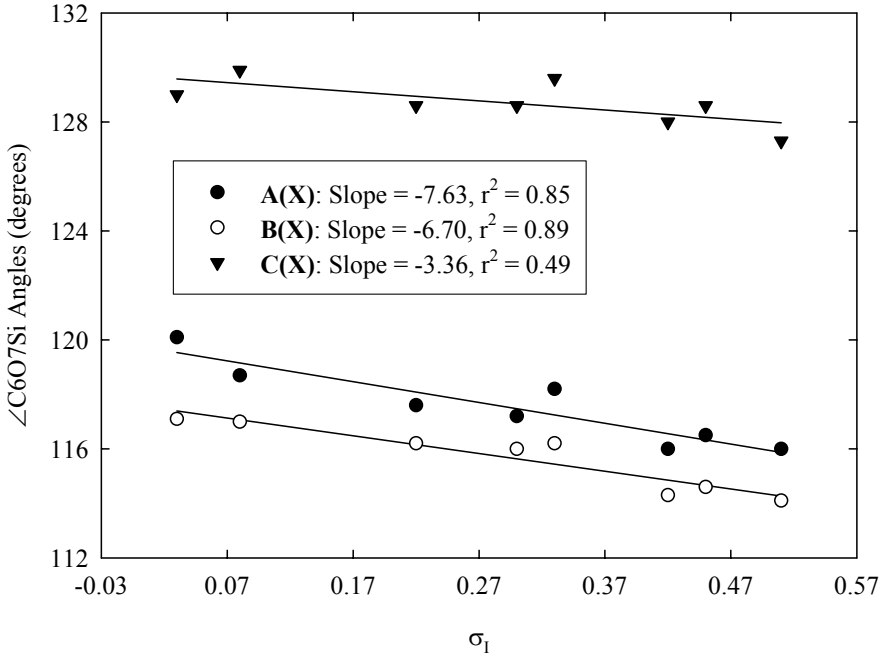

Figure S 1 Plots of the HF/6-311+G(2d,p) calculated ∠C6O7Si angles of the methoxy(substituted-siloxy)carbene conformers versus Swain-Lupton modified Hammett substituent constants.

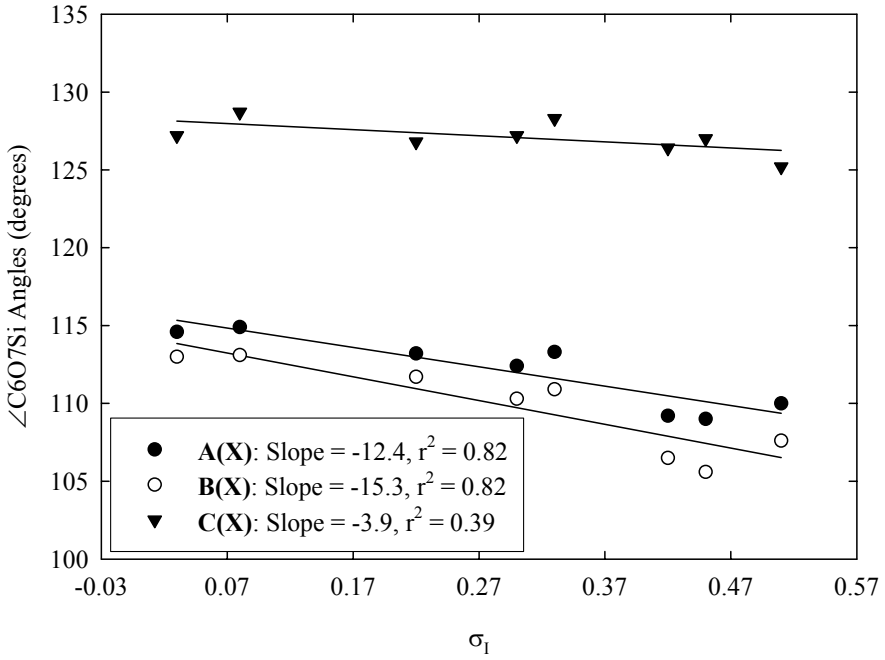

Figure S 2 Plots of the B3LYP/6-311+G(2d,p) calculated ∠C6O7Si angles of the methoxy(substituted-siloxy)carbene conformers versus Swain-Lupton modified Hammett substituent constants.

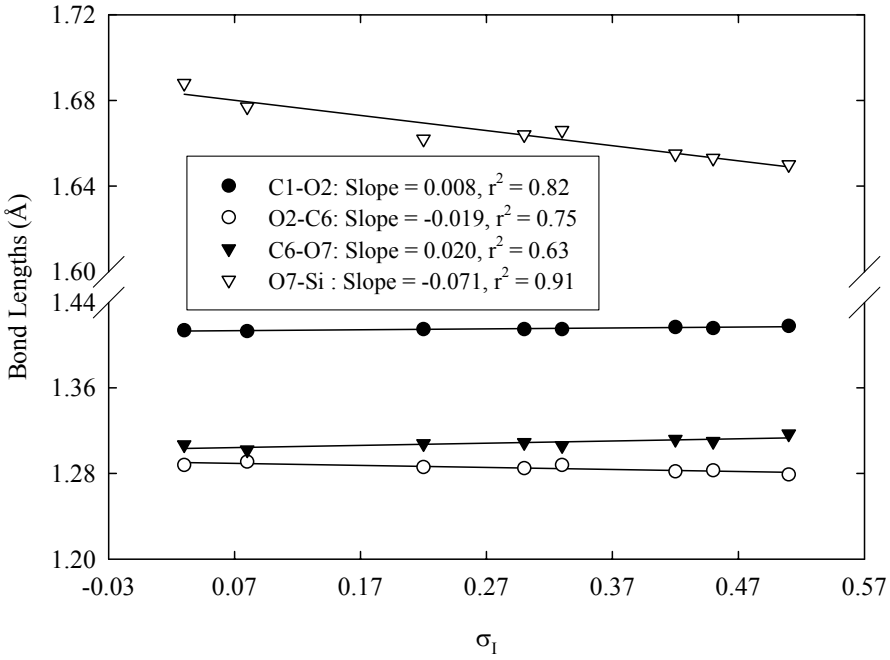

Figure S 3 Plots of the HF/6-311+G(2d,p) bond lengths of conformers **A(X)** of methoxy(substituted-siloxy)carbene versus Swain-Lupton modified Hammett substituent constant σ_I.

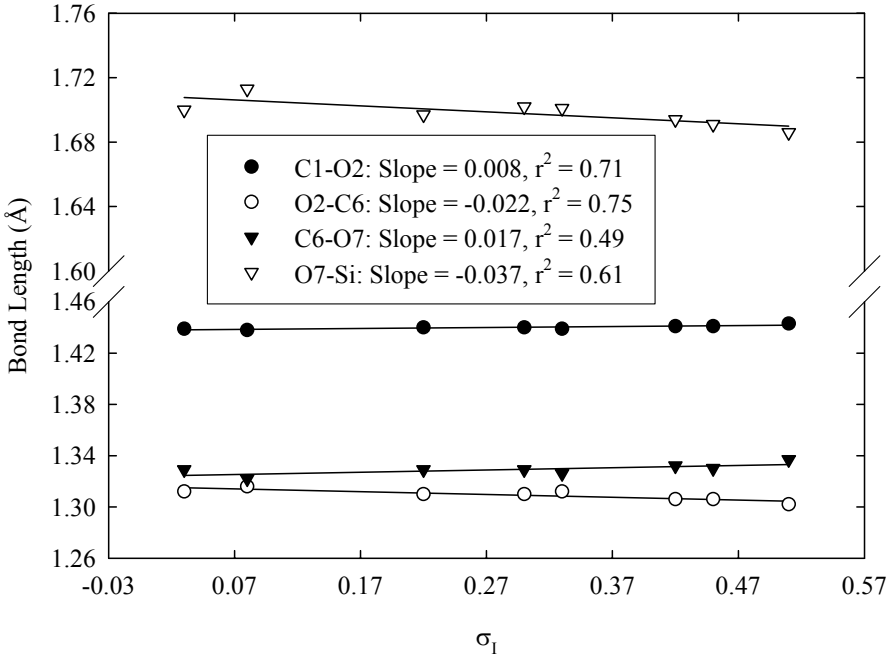

Figure S 4 Plots of the B3LYP/6-311+G(2d,p) bond lengths of conformers **A(X)** of methoxy(substituted-siloxy)carbenes versus Swain-Lupton modified Hammett substituent constant σ_I.

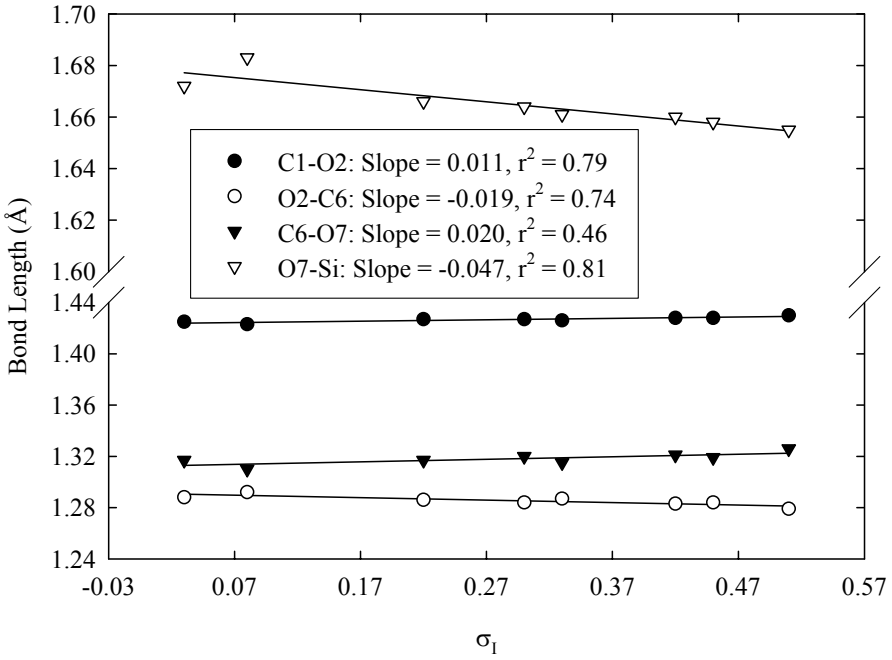

Figure S 5 Plots of the HF/6-311+G(2d,p) bond lengths of conformers **B(X)** of methoxy(substituted-siloxy)carbenes versus Swain-Lupton modified Hammett substituent constant σ_I.

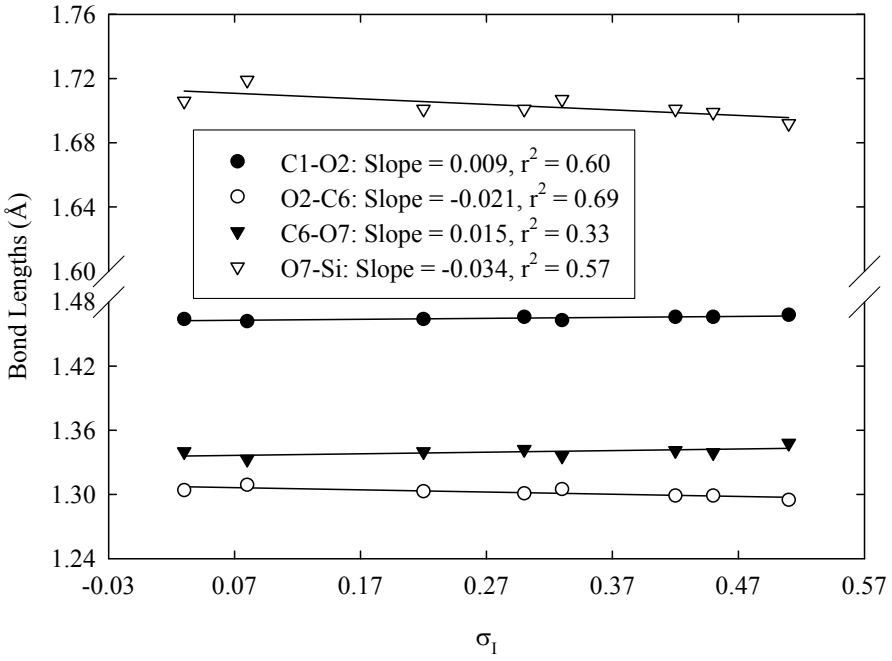

Figure S 6 Plots of the B3LYP/6-311+G(2d,p) bond lengths for conformers **B(X)** of methoxy(substituted-siloxy)carbenes versus Swain-Lupton modified Hammett substituent constant σ_I.

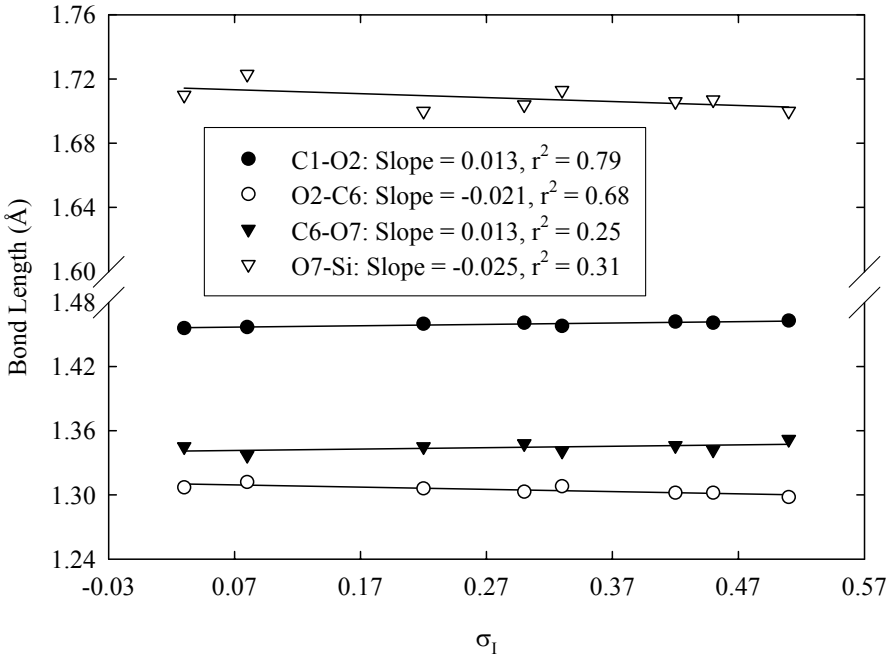

Figure S 7 Plots of the MP2/6-311+G(2d,p) bond lengths for conformers **B(X)** of methoxy(substituted-siloxy)carbenes versus Swain-Lupton modified Hammett substituent constant σ_I.

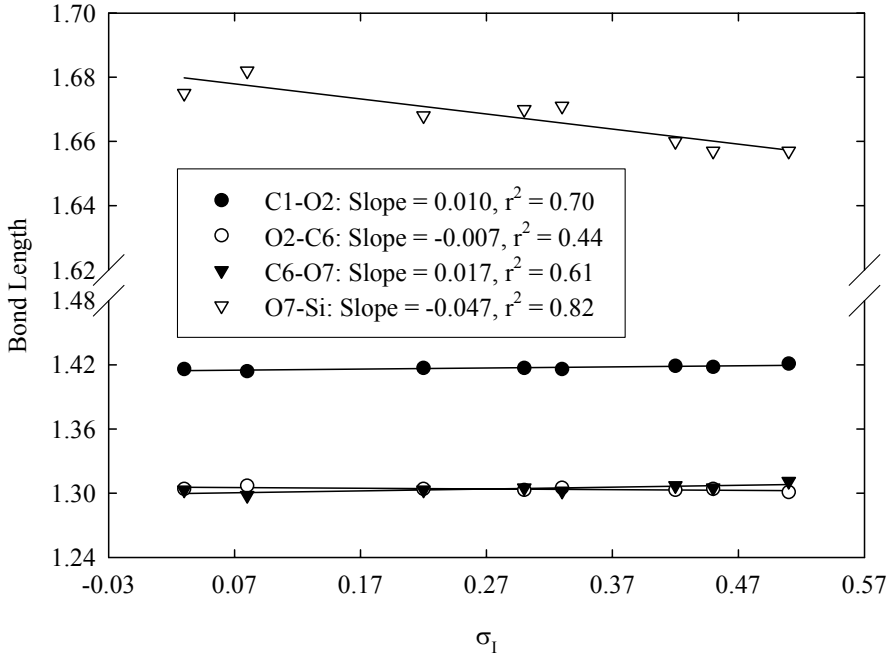

Figure S 8 Plots of the HF/6-311+G(2d,p) bond lengths for conformers **C(X)** of methoxy(substituted-siloxy)carbenes versus Swain-Lupton modified Hammett substituent constant σ_I.

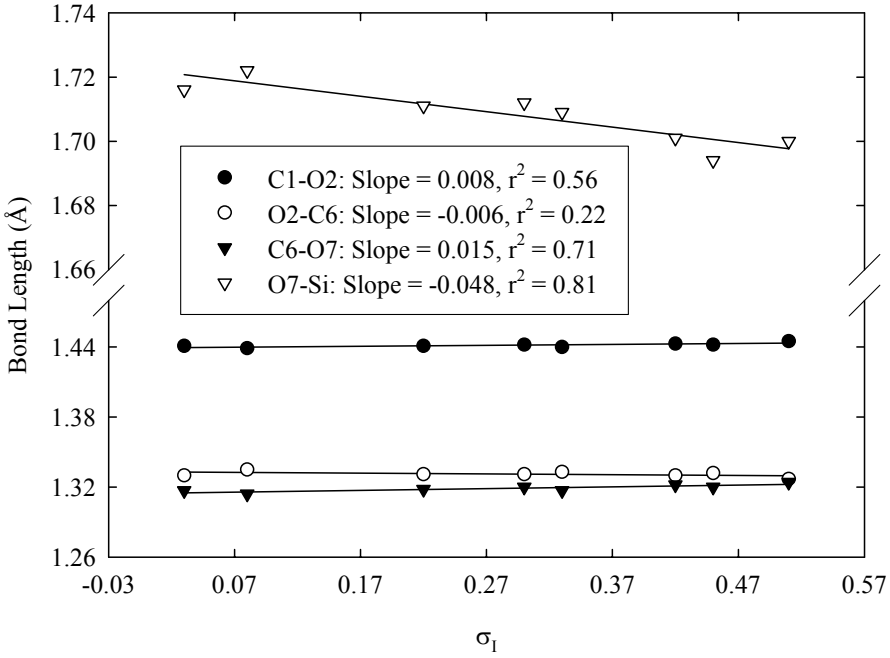

Figure S 9 Plots of the B3LYP/6-311+G(2d,p) bond lengths for conformers **C(X)** of methoxy(substituted-siloxy)carbenes versus Swain-Lupton modified Hammett substituent constant σ_I.

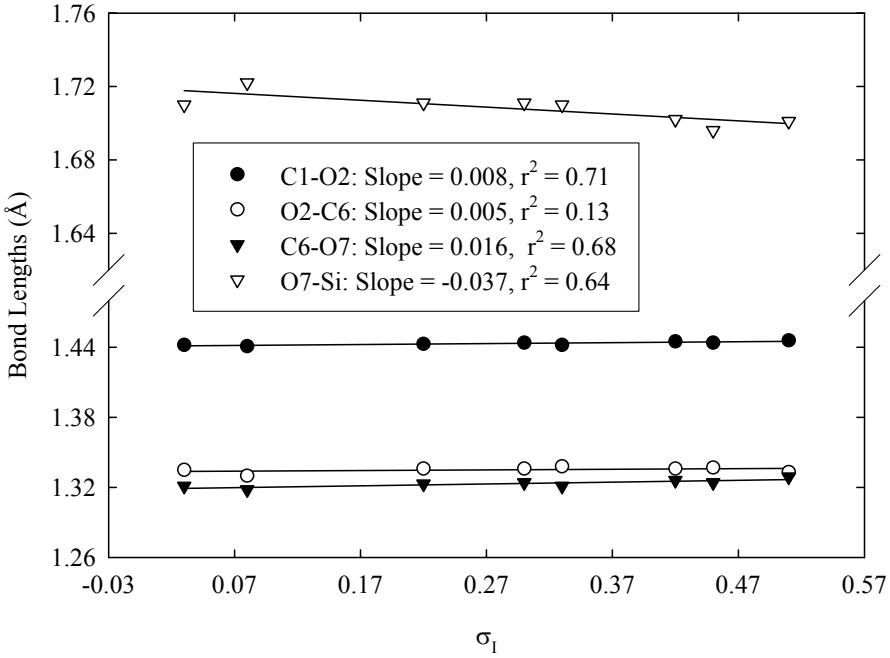

Figure S 10 Plots of the MP2/6-311+G(2d,p) bond lengths for conformers **C(X)** of methoxy(substituted-siloxy)carbenes versus Swain-Lupton modified Hammett substituent constant σ_I.

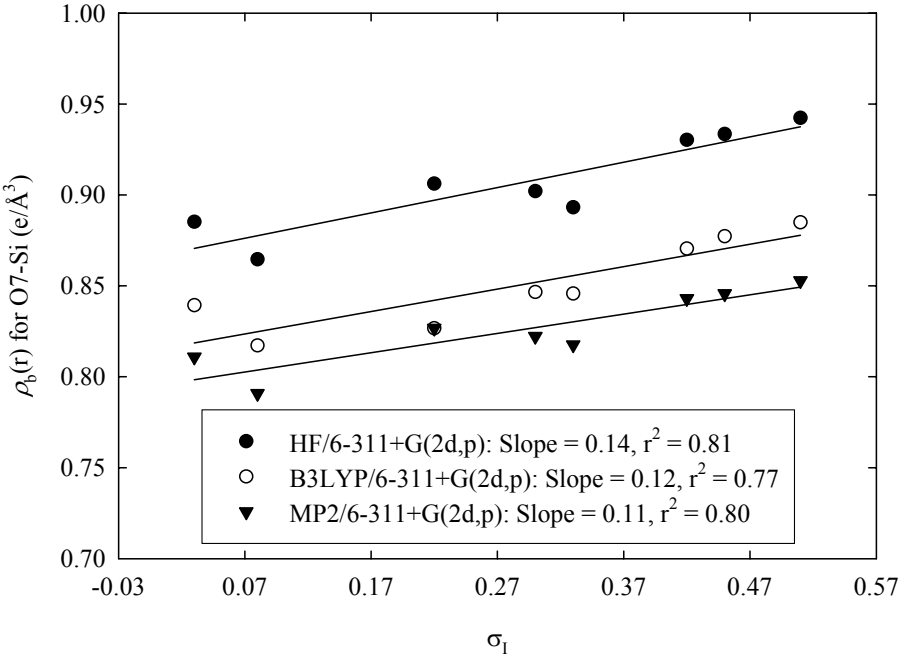

Figure S 11 Dependence of the O7-Si BCP electronic density on Swain-Lupton modified Hammett substituent constants σ_I for conformers **A(X)**.

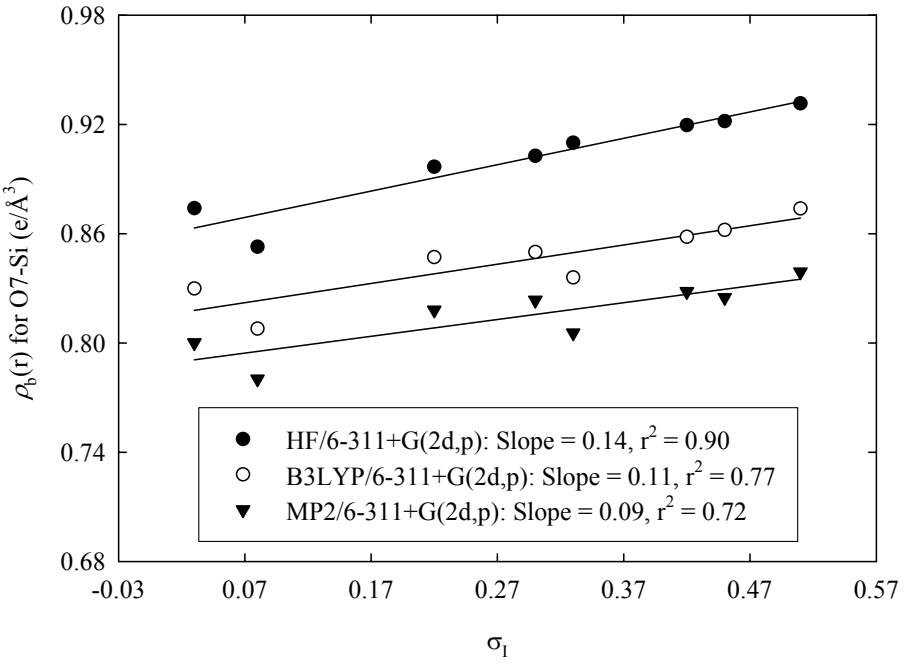

Figure S 12 Dependence of the O7-Si BCP electronic density on Swain-Lupton modified Hammett substituent constants σ_I for conformers **B(X)**.

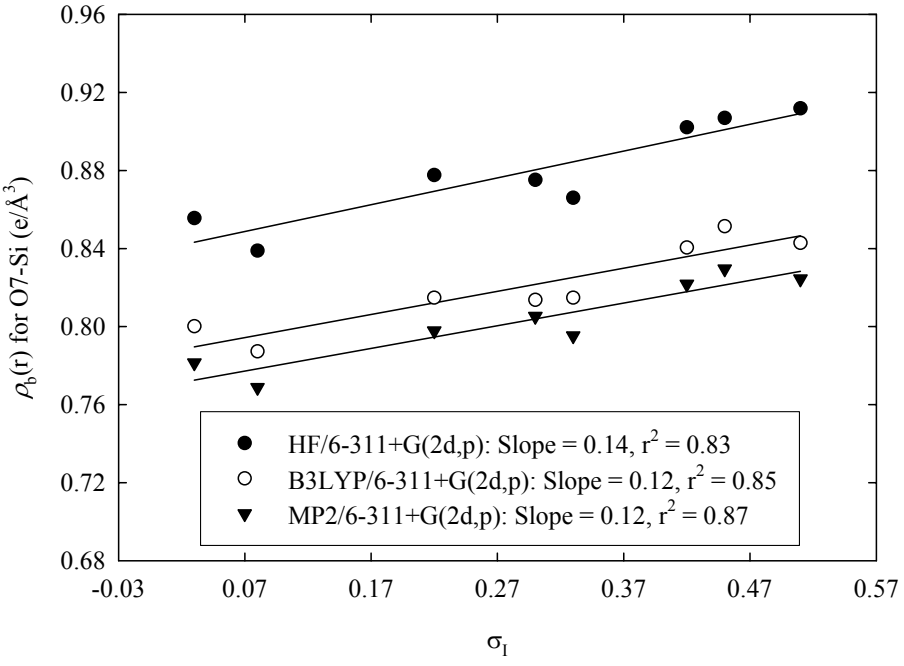

Figure S 13 Dependence of the O7-Si BCP electronic density on Swain-Lupton modified Hammett substituent constants σ_I for conformers **C(X)**.

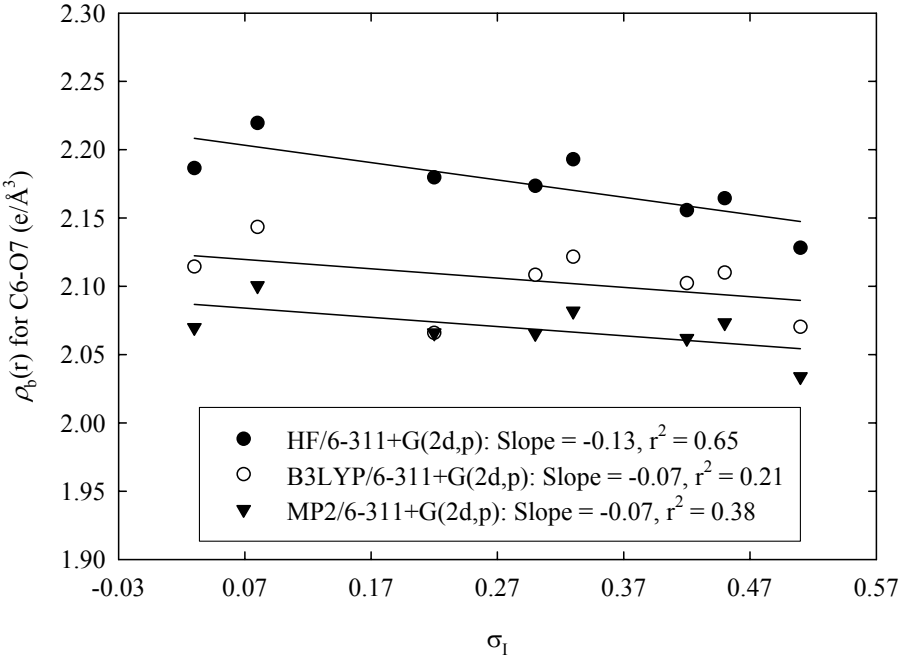

Figure S 14 Dependence of the C6-O7 BCP electronic density on Swain-Lupton modified Hammett substituent constants σ_I for conformers **A(X)**.

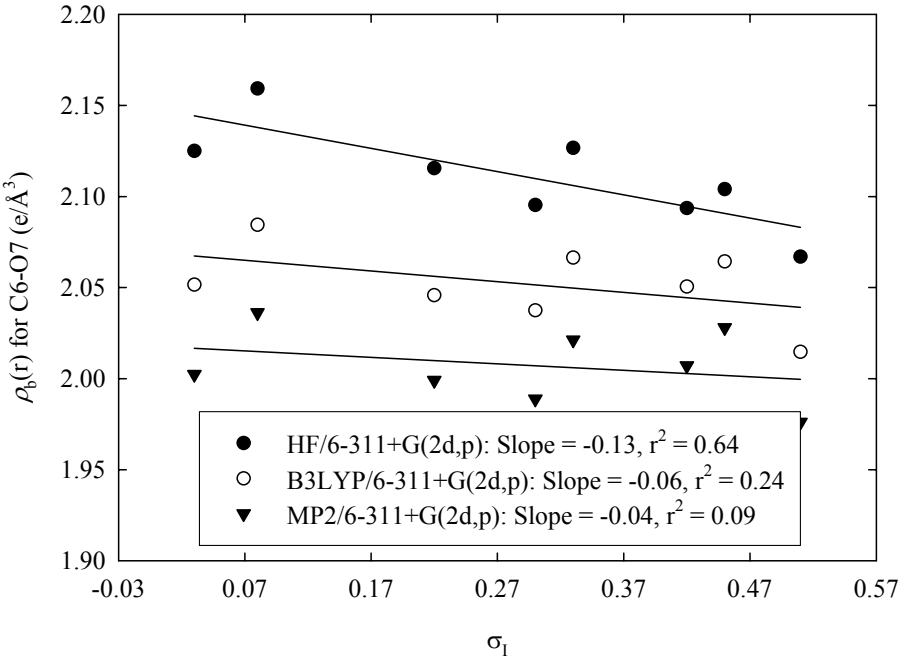

Figure S 15 Dependence of the C6-O7 BCP electronic density on Swain-Lupton modified Hammett substituent constants σ_I for conformers **B(X)**.

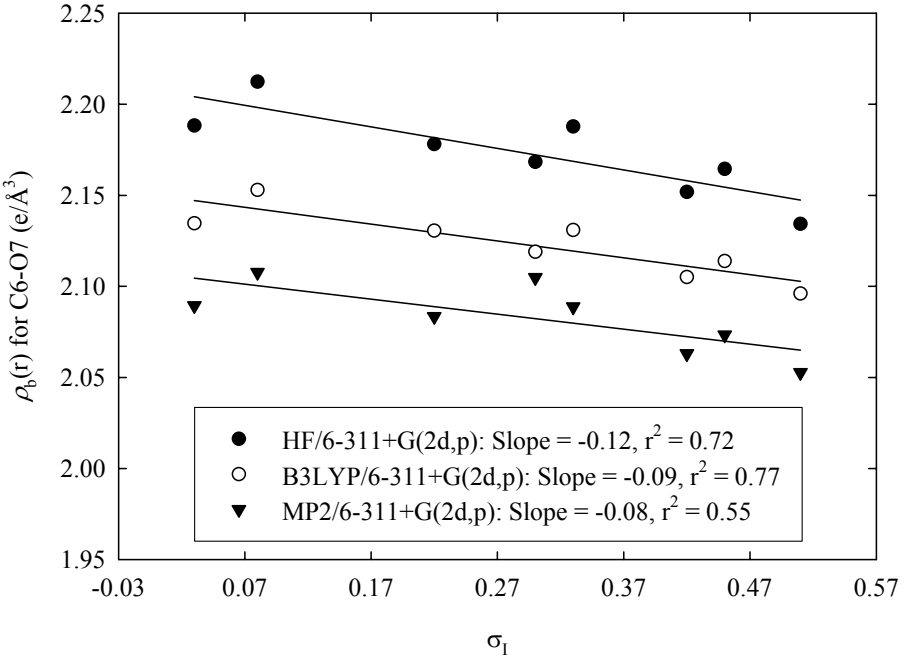

Figure S 16 Dependence of the C6-O7 BCP electronic density on Swain-Lupton modified Hammett substituent constants σ_I for conformers **C(X)**.

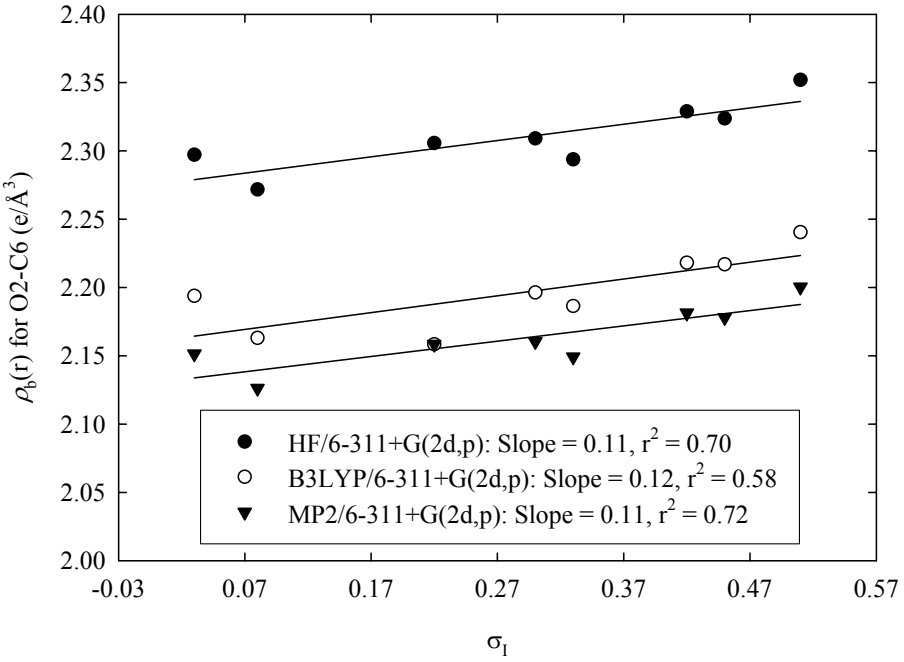

Figure S 17 Dependence of the O2-C6 BCP electronic density on Swain-Lupton modified Hammett substituent constants σ_I for conformers **A(X)**.

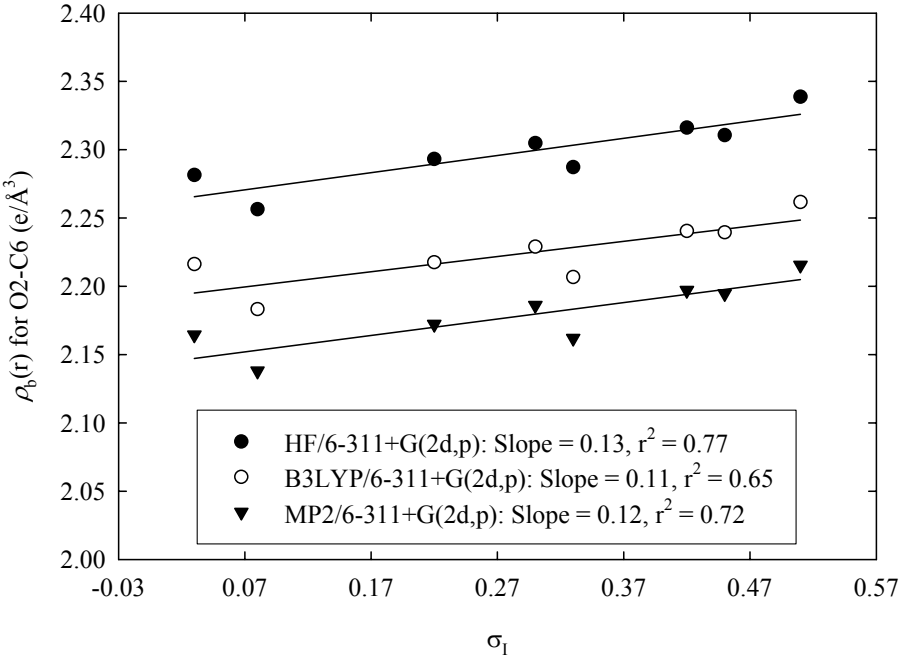

Figure S 18 Dependence of the O2-C6 BCP electronic density on Swain-Lupton modified Hammett substituent constants σ_I for conformers **B(X)**.

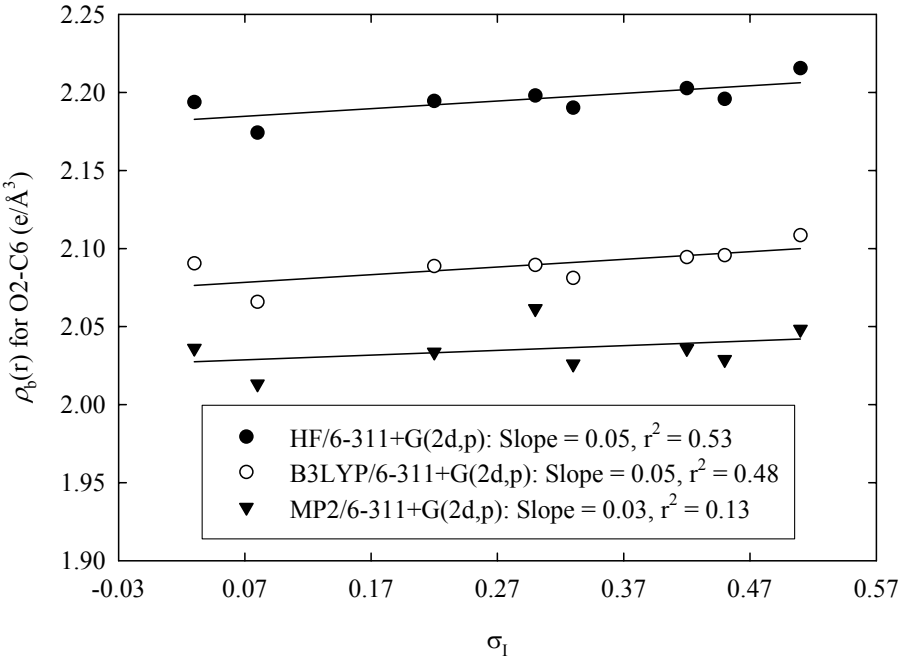

Figure S 19 Dependence of the O2-C6 BCP electronic density on Swain-Lupton modified Hammett substituent constants σ_I for conformers **C(X)**.

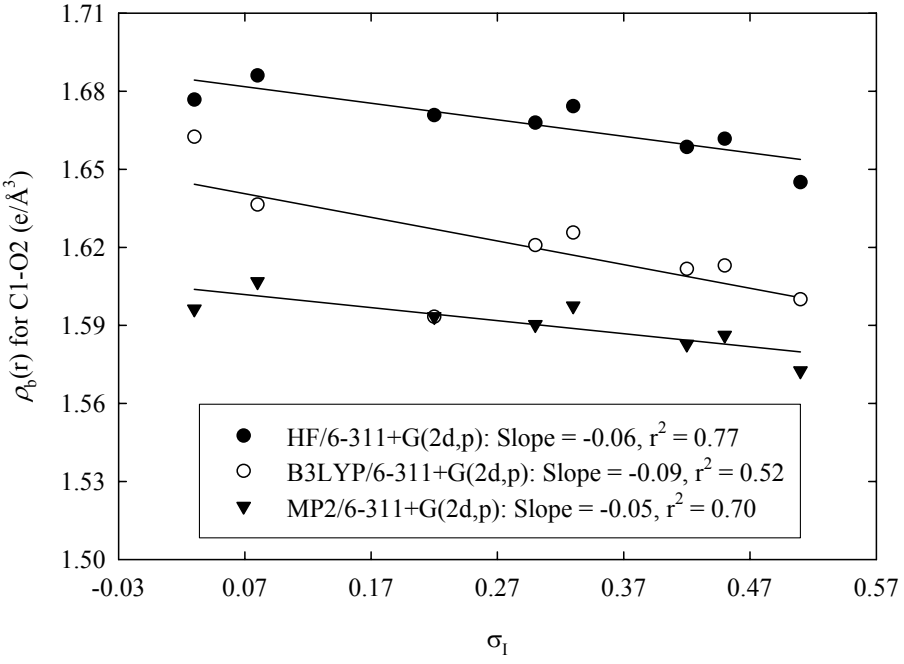

Figure S 20 Dependence of the C1-O2 BCP electronic density on Swain-Lupton modified Hammett substituent constants σ_I for conformers **A(X)**.

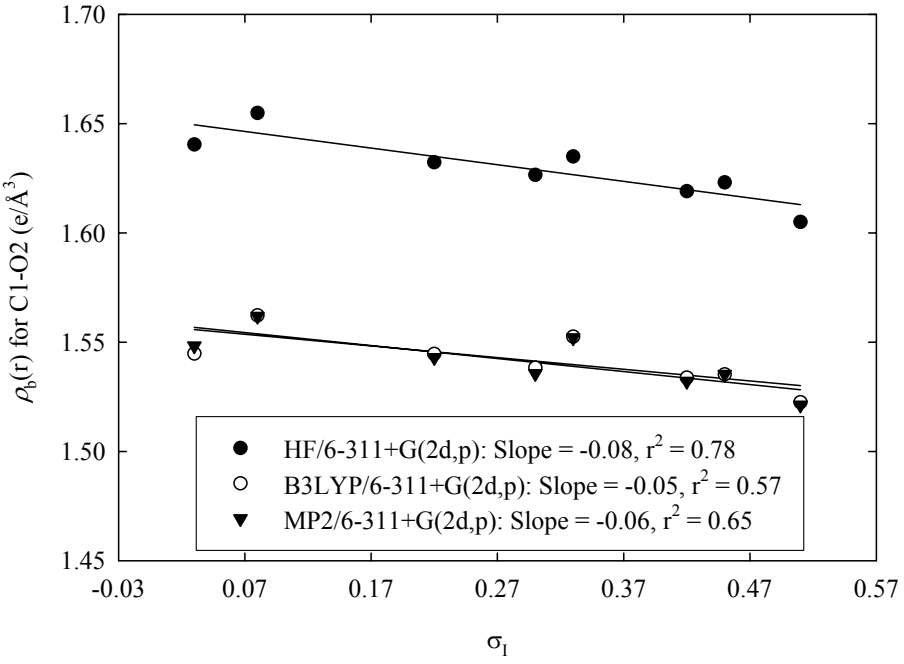

Figure S 21 Dependence of the C1-O2 BCP electronic density on Swain-Lupton modified Hammett substituent constants σ_I for conformers **B(X)**.

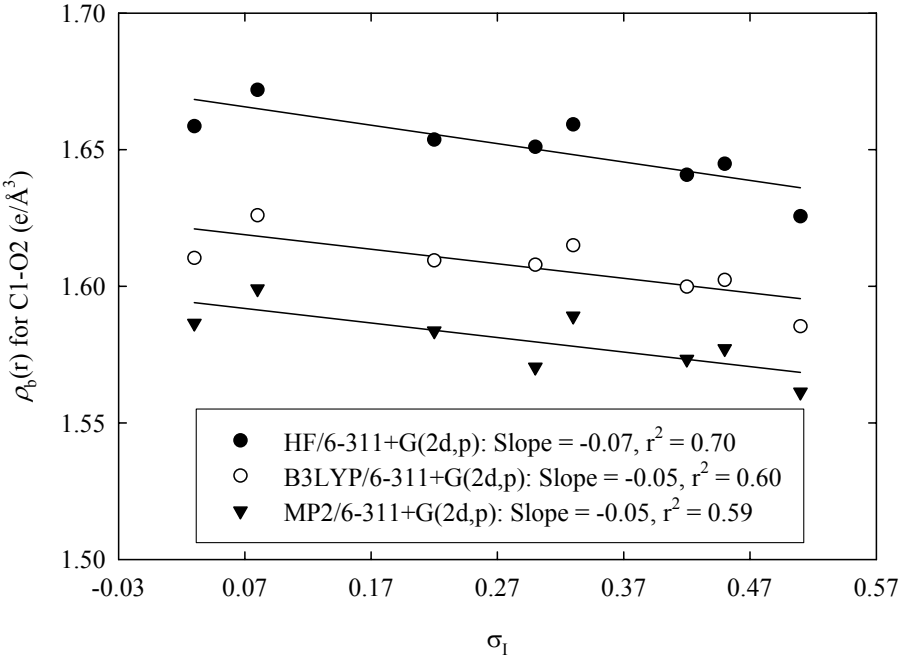

Figure S 22 Dependence of the C1-O2 BCP electronic density on Swain-Lupton modified Hammett substituent constants σ_I for conformers **C(X)**.

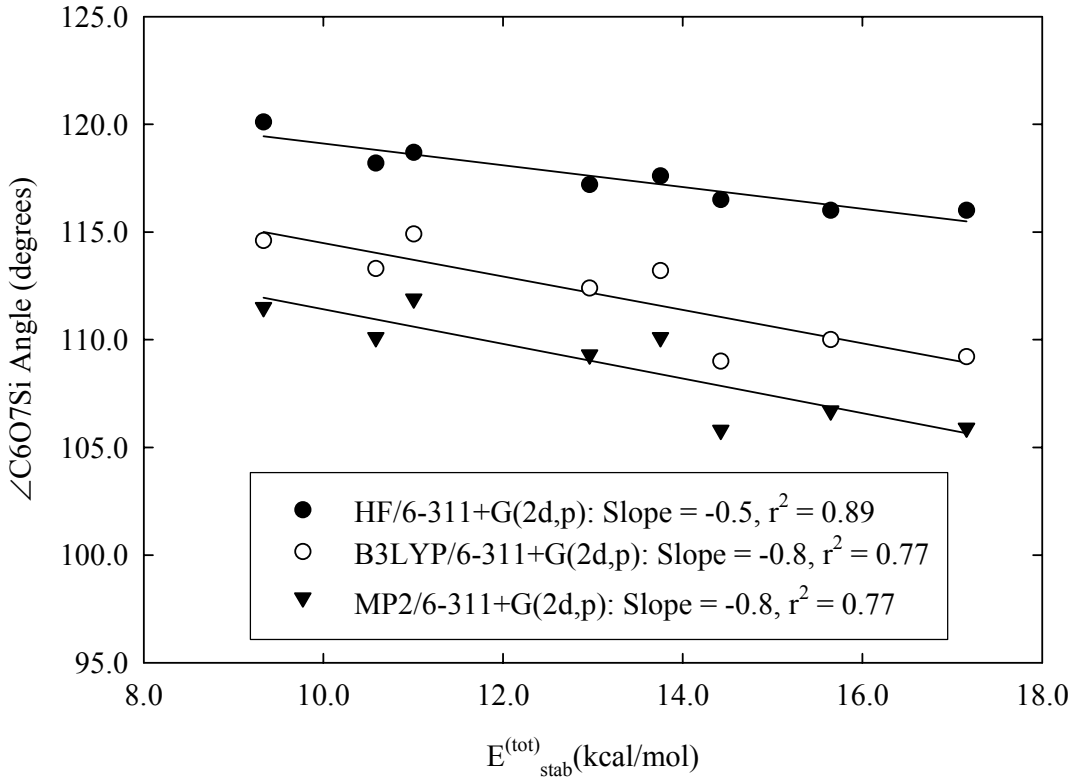

Figure S 23 Plots of the ∠C6O7Si angles of conformers **A(X)** versus stabilization energies $E^{(tot)}_{stab}$ due to hyperconjugation.

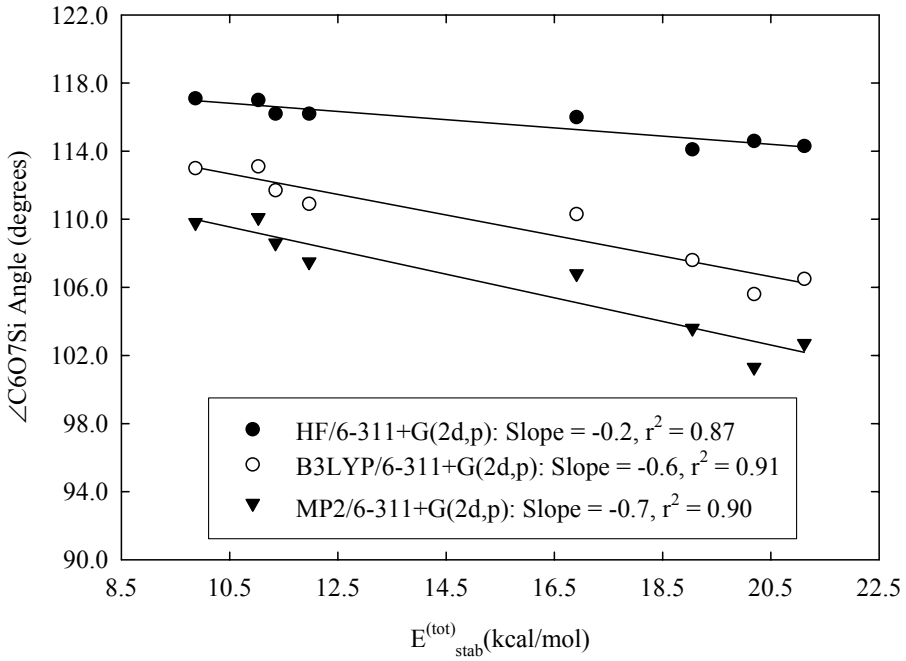

Figure S 24 Plots of the ∠C6O7Si angles of conformers **B(X)** versus stabilization energies $E^{(tot)}_{stab}$ due to hyperconjugation.

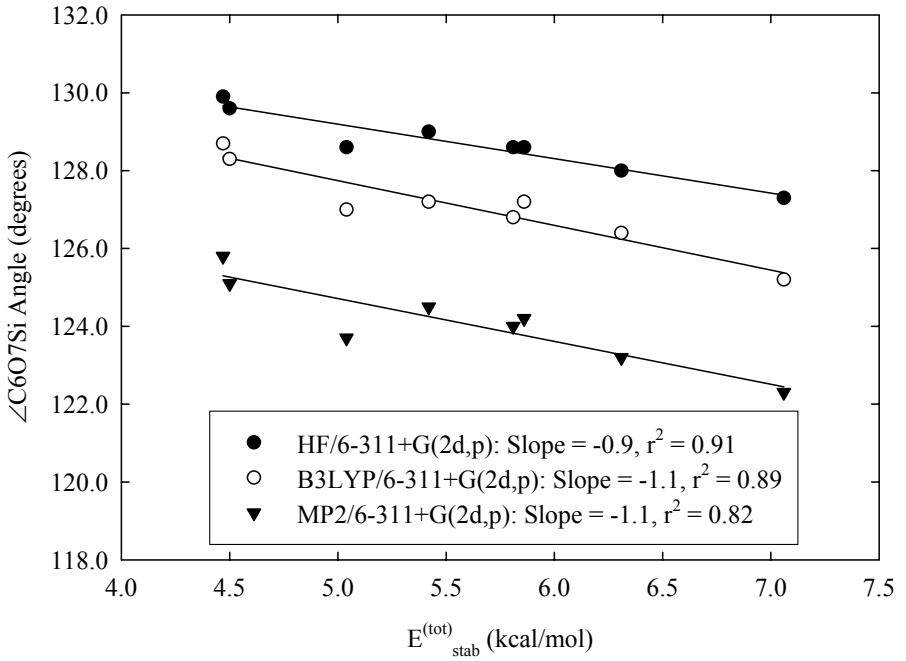

Figure S 25 Plots of the ∠C6O7Si angles for conformers **C(X)** versus stabilization energies $E^{(tot)}_{stab}$ due to hyperconjugation.

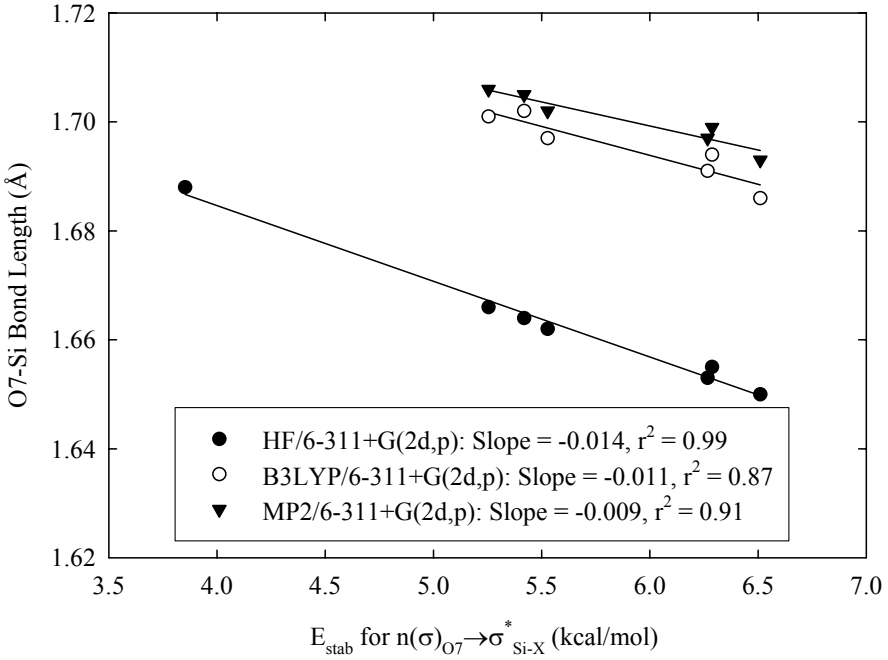

Figure S 26 Plots of the O7-Si bond length versus stabilization energies E_{stab} due to $n(\sigma)_{O7} \rightarrow \sigma^*_{Si\text{-}X}$ hyperconjugation in conformers **A(X)**. Note that E_{stab} also includes $n(\sigma)_{O7} \rightarrow RY^*_{Si}$ interactions.

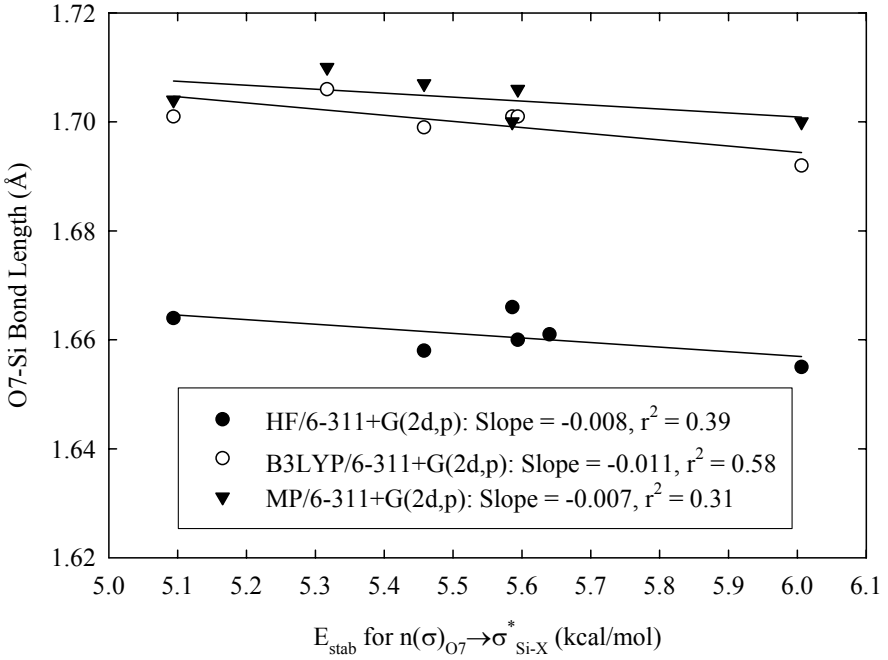

Figure S 27 Plots of the O7-Si bond length versus stabilization energies E_{stab} due to $n(\sigma)_{O7} \rightarrow \sigma^*_{Si\text{-}X}$ hyperconjugation in conformers **B(X)**. Note that E_{stab} also includes $n(\sigma)_{O7} \rightarrow RY^*_{Si}$ interactions.

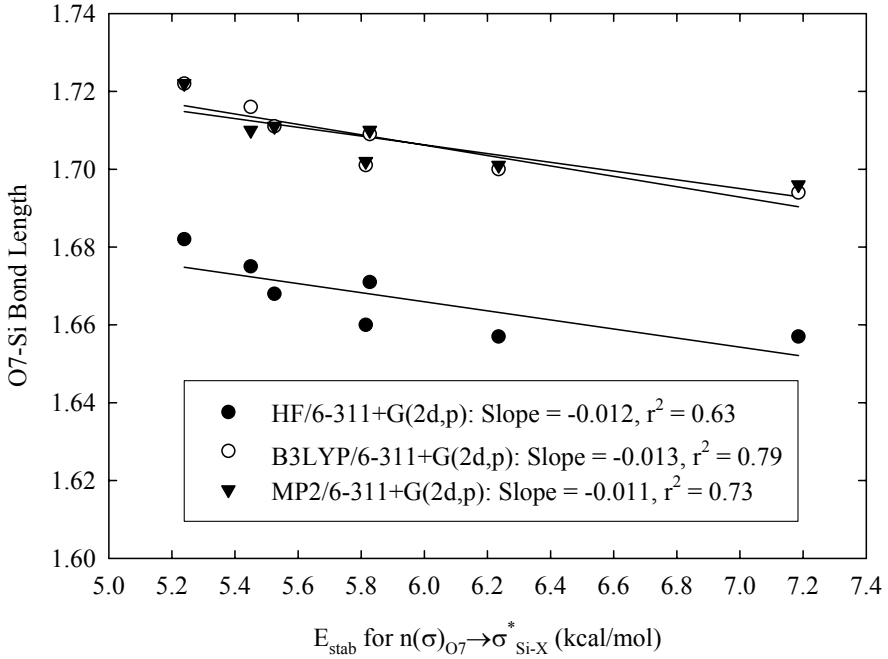

Figure S 28 Plots of the O7-Si bond length versus stabilization energies E_{stab} due to $n(\sigma)_{O7} \rightarrow \sigma^*_{Si\text{-}X}$ hyperconjugation in conformers **C(X)**. Note that E_{stab} also includes $n(\sigma)_{O7} \rightarrow RY^*_{Si}$ interactions.

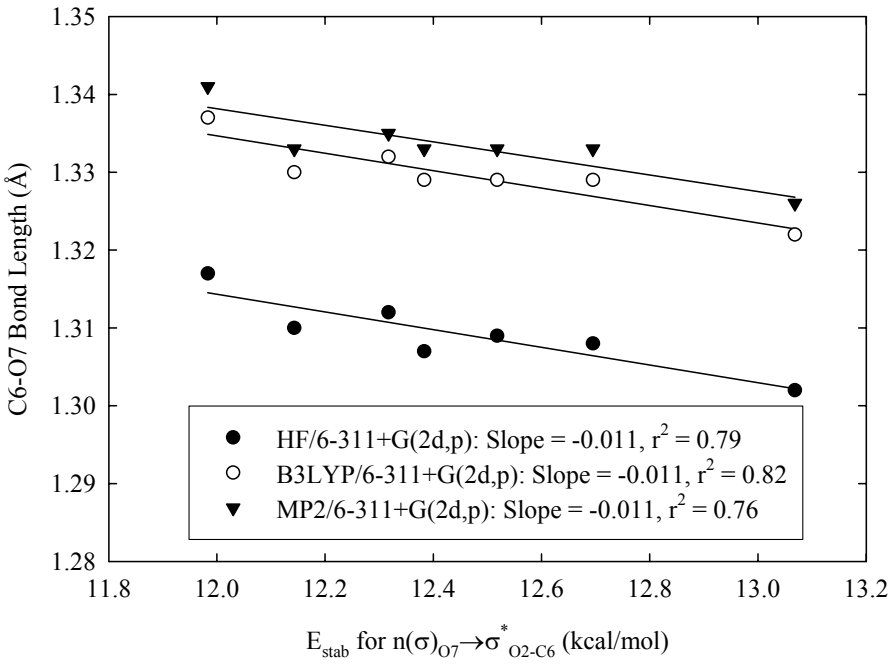

Figure S 29 Plots of the C6-O7 bond length versus stabilization energies E_{stab} due to $n(\sigma)_{O7} \rightarrow \sigma^*_{O2\text{-}C6}$ hyperconjugation in conformers **A(X)**. Note that E_{stab} also includes $n(\sigma)_{O7} \rightarrow RY^*_{C6}$ interactions.

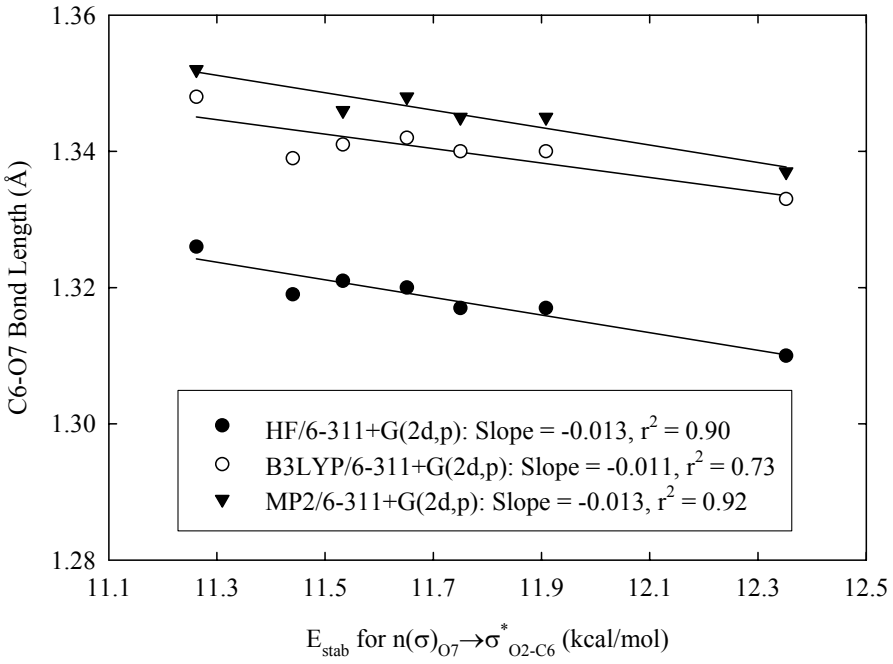

Figure S 30 Plots of the C6-O7 bond length versus stabilization energies E_{stab} due to $n(\sigma)_{O7} \rightarrow \sigma^*_{O2\text{-}C6}$ hyperconjugation in conformers **B(X)**. Note that E_{stab} also includes $n(\sigma)_{O7} \rightarrow RY^*_{C6}$ interactions.

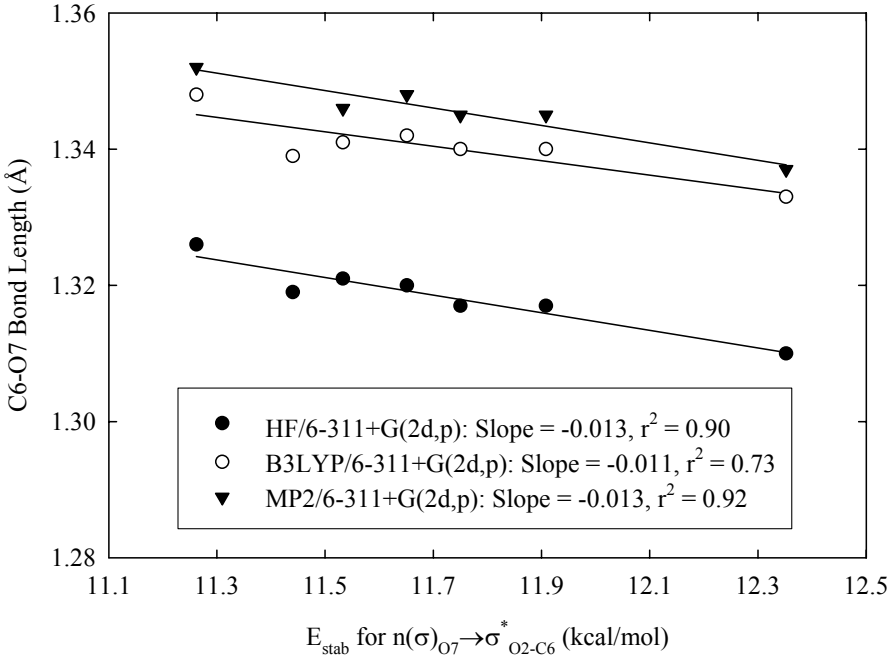

Figure S 31 Plots of the C6-O7 bond length versus stabilization energies E_{stab} due to $n(\sigma)_{O7} \rightarrow \sigma^*_{O2\text{-}C6}$ hyperconjugation in conformers **C(X)**. Note that E_{stab} also includes $n(\sigma)_{O7} \rightarrow RY^*_{C6}$ interactions.

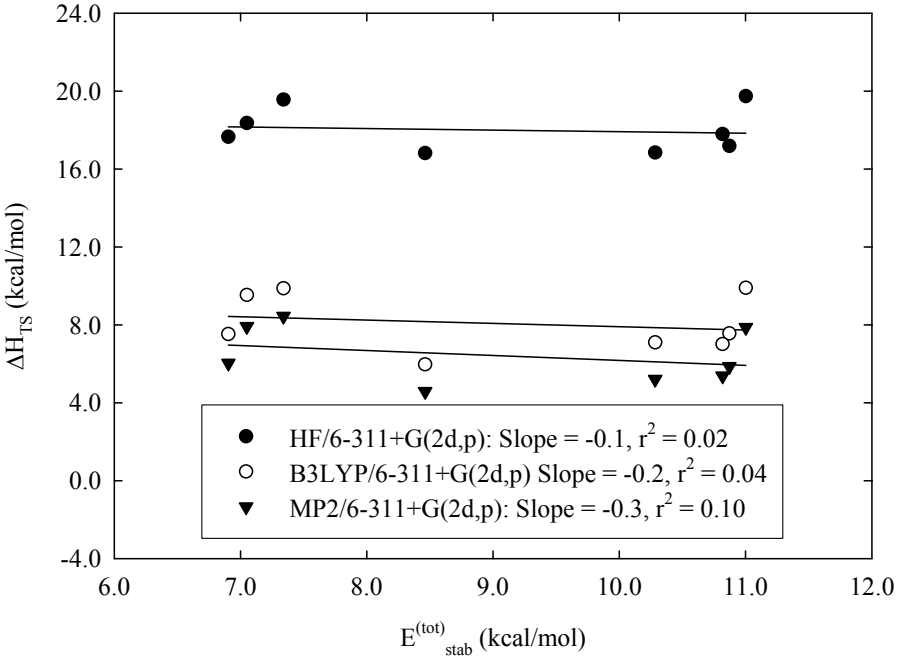

Figure S 32 Plots of activation enthalpies for 1,2-silyl migration versus computed HF/6-311+G(2d,p) stabilization energies due to hyperconjugation in conformers **A(X)**.

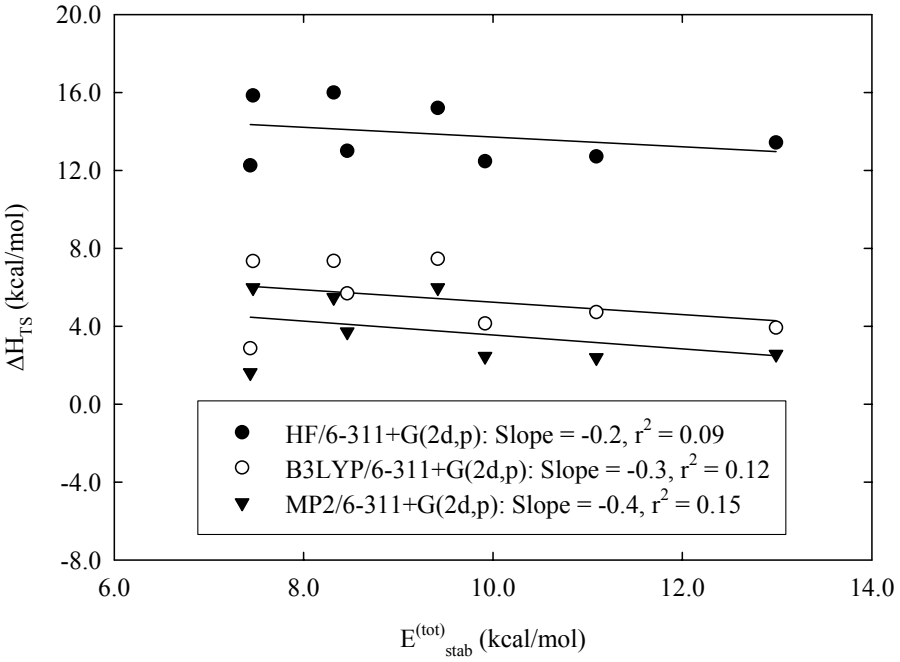

Figure S 33 Plots of activation enthalpies for 1,2-silyl migration versus computed HF/6-311+G(2d,p) stabilization energies due to hyperconjugation in conformers **B(X)**.

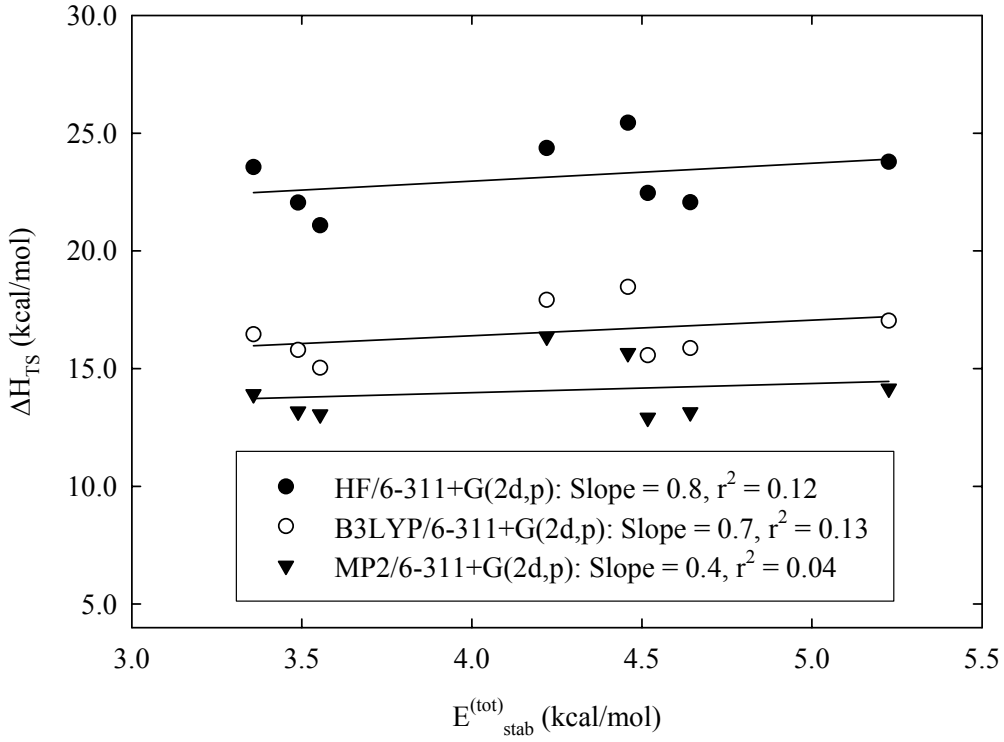

Figure S 34 Plots of activation enthalpies for decarbonylation versus computed HF/6-311+G(2d,p) stabilization energies due to hyperconjugation in conformers **C(X)**.

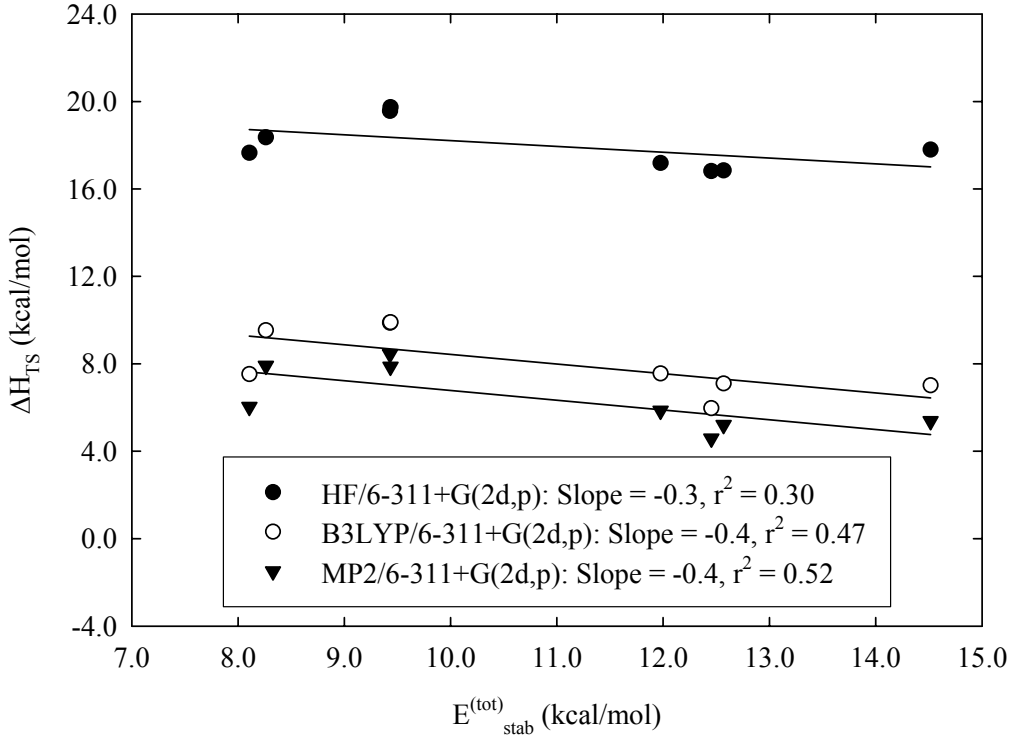

Figure S 35 Plots of activation enthalpies for 1,2-silyl migration versus computed B3LYP/6-311+G(2d,p) stabilization energies due to hyperconjugation in conformers **A(X)**.

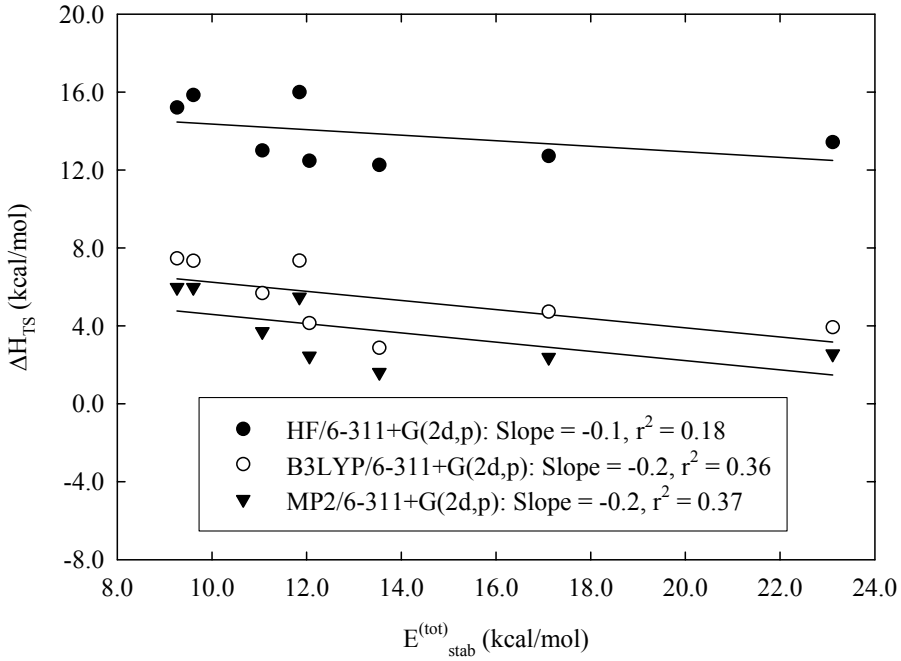

Figure S 36 Plots of activation enthalpies for 1,2-silyl migration versus computed B3LYP/6-311+G(2d,p) stabilization energies due to hyperconjugation in conformers **B(X)**.

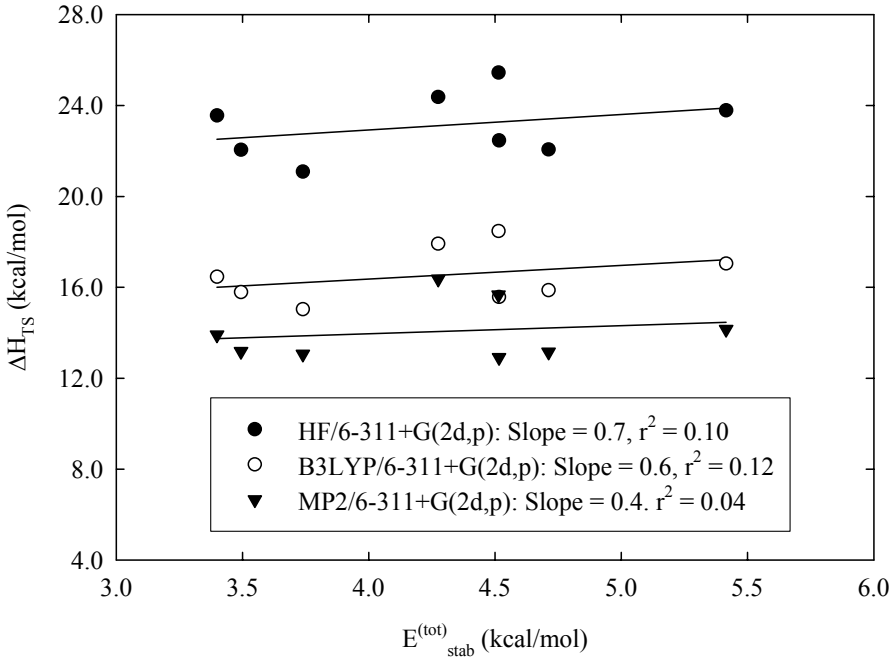

Figure S 37 Plots of activation enthalpies for decarbonylation versus computed B3LYP/6-311+G(2d,p) stabilization energies due to hyperconjugation in conformers C(X).